Surface and Interference Coenhanced Raman Scattering of Graphene

Libo Gao,[†] Wencai Ren,[†,*] Bilu Liu,[†] Riichiro Saito,[‡] Zhong-Shuai Wu,[†] Shisheng Li,[†] Chuanbin Jiang,[†] Feng Li,[†] and Hui-Ming Cheng[†,*]

[†]Shenyang National Laboratory for Materials Science, Institute of Metal Research, Chinese Academy of Sciences, 72 Wenhua Road, Shenyang 110016, People's Republic of China, and [‡]Department of Physics, Tohoku University, Sendai 980-8578, Japan

ABSTRACT We propose a novel surface and interference coenhanced Raman scattering technique to dramatically enhance the Raman signal intensity of graphene by using a specifically designed substrate of Si capped with surface-active metal and oxide double layers (SMO). The total enhancement ratio can reach the order of 10^3 compared with the original Si substrate. Combining the visibility of graphene on the SMO substrate, we demonstrate that the tiny structure change and surface structure of graphene can be easily detected. This technique makes Raman spectroscopy a more powerful tool in the field of ultrasensitive characterization of graphene, isolated carbon nanotubes, and other film-like materials.

KEYWORDS: graphene · Raman scattering · surface · interference · enhancement

G raphene, as a perfect two-dimensional carbon system, has attracted increasing attention as a promising candidate for future electronics because of its unique structure, high crystal quality, ballistic transport under ambient condition, and the massless Dirac fermion-like charge carriers.[1−4] It has been envisioned that future electronic circuits could be made up of graphene-based field-effect transistors and conductive interconnects with high mobility of charge carriers.[3] In addition, graphene also exhibits great promise for potential applications in many other technological fields such as sensors,[5] composites,[6] transistors,[7] transparent conductive films,[8] and solar cells.[9] However, the properties of graphene are very sensitive to its fine structure, including the number of layers, edge structures, defects, doping, *etc*. Therefore, detecting these structural characteristics and investigating their influence on the properties of graphene are crucial both for the structural modulation and further applications of graphene.

Raman spectroscopy offers a powerful tool to probe the structural characteristics[10−12] and properties[13−21] of graphene. The number of graphene layers can be easily identified by the profile and position of the Raman second order (2D) band and the shift of G band frequency.[10−12] It has also been demonstrated that the Raman spectra can be used to determine and monitor the electron/hole dopants in graphene,[13−17] the electronic structure of bilayer graphene can be probed by resonant Raman scattering,[18] and the thermal conductivity and strain of graphene can be extracted from the shift of G band and 2D band frequency.[19−21] However, for graphene, a one-atom-thick flat allotrope of carbon, much of the incident light is transmitted[22] and only a small portion is used to generate scattered radiation during Raman measurements. Moreover, unlike carbon nanotubes,[23] it is not expected for graphene to satisfy strong resonant Raman scattering conditions because of no singular density of states and no exciton formation of graphene at room temperature, even though one always gets the resonance condition for any excitation energies of light. As a result, Raman signals of graphene are very weak, even undetectable on many substrates. Consequently, some fine structural characteristics, such as a low concentration of defects, vacancies, doping, functional groups, crumpling, and edge structures, cannot be sensitively probed and well-distinguished from the weak Raman spectra of graphene. *In situ* Raman measurements can monitor the structural evolution of graphene during its growth process and property evaluation, or under external fields, which will provide some useful information on the structural and property modulation of graphene. However, the weak Raman signals prevent investigations on the time-dependent structural evolution since no sufficient Raman signals can be obtained on the time scale of the studied processes. Therefore, enhancing the Raman signals of graphene is essentially
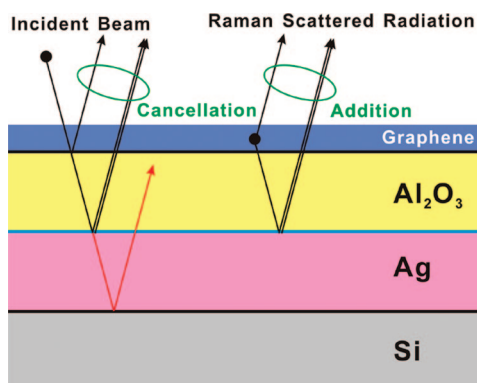
Figure 1. Schematic of laser penetrating through a typical SMO substrate of Si/Ag/Al$_2$O$_3$ with graphene on it.

important for their controllable synthesis, detailed structural characterization, and property modulation.

Currently, the effect of substrate on Raman spectra of graphene has been widely investigated,[24−26] and Si substrate capped with a specific thickness of oxides, such as Si/SiO$_2$ and Si/Al$_2$O$_3$, is usually used for optical observations[4,27,28] and to enhance the Raman signals of graphene utilizing so-called interference-enhanced Raman scattering (IERS) technique.[29−32] Generally, a substrate consisting of a transparent dielectric film resting on an opaque metallic reflector is used to generate IERS of a very thin film sample. By adjusting the thickness of the dielectric film, an IERS condition can be established: all of the incident intensity is absorbed, the scattered radiation suffers from relatively little reab-

sorption in the thin sample, and an in-phase addition of the emitted radiation is created. By using the IERS technique, an enhancement ratio of ∼30 is achieved for graphene located on a Si/SiO$_2$ substrate.[32] Surface-enhanced Raman scattering (SERS) is another spectroscopic technique, which combines modern laser spectroscopy with the exciting optical properties of metallic nanostructures and provides an effective way to dramatically enhance the Raman signals of molecules attached to the nanometer-sized metal structures.[33−36] Combining with ultrasensitive detection limit, high spatial resolution, trace analytical capability, and high structural selectivity, SERS has been widely used for the ultrasensitive detection and characterization of various single molecules and carbon nanotubes.[33,34] In this article, taking advantage of both the IERS and SERS techniques, we proposed and developed a surface and interference coenhanced Raman scattering (SICERS) technique to significantly enhance the Raman signals of graphene by using a specifically designed substrate of Si/SERS active metal/oxide layer (SMO). Surprisingly, the total enhancement ratio for graphene can reach more than 10 times and the order of 10^2 compared with that by using the sole IERS or SERS technique. Moreover, the graphene is visible on these SMO substrates, and this is good for the location during the Raman measurements. We also demonstrated that the tiny structure change of graphene on the substrate and the surface structures of graphene can be easily probed by utilizing this technique.

RESULTS AND DISCUSSION

In order to evaluate the enhancement effect of the SMO substrate, we analyzed the penetrating process of incident laser through a typical SMO substrate, Si/Ag/Al$_2$O$_3$, and the schematic is shown in Figure 1. According to the SERS mechanism,[35] the collective excitation of the electron gas of a conductor (here Ag film), that is, surface plasmon, is confined near the interface of Ag/Al$_2$O$_3$, and the electromagnetic field of the light at the interface is greatly enhanced under the conditions of surface plasmon excitation.[36] Therefore, the incident and reflected radiations at the interface of Ag/Al$_2$O$_3$ are enhanced. According to IERS mechanism, both the surface-enhanced reflected radiation and the incident radiation contribute to the total Raman scat-
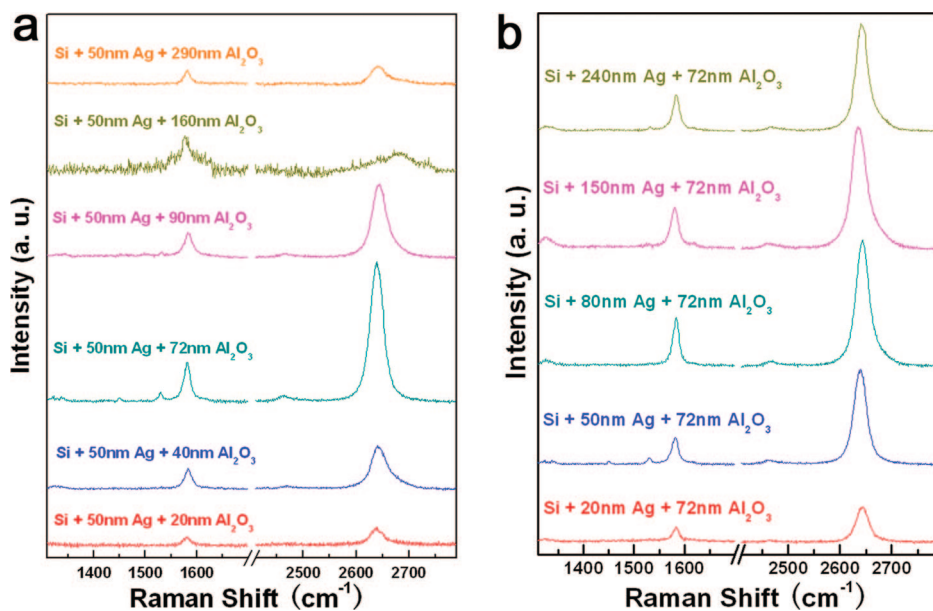

Figure 2. Enhancement effect comparison of graphene on different substrates. (a) Raman spectra of graphene on a Si substrate with 50 nm thick Ag film and different thickness of Al$_2$O$_3$ layers, revealing that the enhancement changes dramatically with the Al$_2$O$_3$ thickness. Note that we used the Raman spectra of few-layer (<5) graphene instead of monolayer on the substrate of Si/50 nm Ag/160 nm Al$_2$O$_3$ since the Raman signals of monolayer graphene are too weak in this case. (b) Raman spectra of graphene on a Si substrate with 72 nm thick Al$_2$O$_3$ layer and different thicknesses of Ag film, revealing that the enhancement effects are increased by increasing the thickness of Ag film from 20 to 80 nm and then saturates when Ag thickness is 150 and 240 nm. All the Raman spectra were taken at a laser power of about 1 mW and short collection time of 120 s except the substrate of Si/50 nm Ag/160 nm Al$_2$O$_3$ (about 10 mW of 1800 s).

tering process in the IERS system. As a consequence, a stronger SICERS process shall occur on the SMO substrate compared with the conventional IERS and SERS processes, and thus we call it the SICERS technique.

According to the IERS mechanism, the thickness of the Al_2O_3 layer plays the key role in establishing the IERS condition. On the other hand, by increasing the thickness of Ag film, the reflected light at the interface of Ag/Al_2O_3 will increase and then reach the maximum. Consequently, the Raman signals of graphene will become stronger and then saturate at a certain Ag thickness. Therefore, the thicknesses of Ag and Al_2O_3 layers in the SMO substrate are required to be optimized to maximize the Raman enhancement of graphene. We investigated the influence of the thickness of Ag and Al_2O_3 layers on the Raman intensities of graphene. The enhancement changes dramatically with the thickness of the Al_2O_3 layer for the SMO substrates with a 50 nm thick Ag layer (Figure 2a). The enhancement ratio reaches the maximum value with a ~72 nm thick Al_2O_3 layer, and this value is also consistent with that suitable for optical observation of graphene.[27] For the SMO substrates with a 72 nm thick Al_2O_3 layer (Figure 2b), the enhancement ratio increases significantly with an increase of the thickness of Ag layer from 20 to 80 nm and then saturates when the Ag thickness is increased to 150 and 240 nm. It is worth noting that these results are qualitatively in agreement with the above analyses.

Figure 3 shows the Raman spectra of graphene on different kinds of substrates. We find that the Raman intensities of monolayer graphene are dramatically enhanced on the optimized SMO substrates (Si/50 nm Ag/72 nm Al_2O_3 and Si/50 nm Au/72 nm Al_2O_3) compared with all those on the corresponding IERS substrate (Si/72 nm Al_2O_3), SERS substrate (Si/50 nm Ag), and an original Si substrate (without oxide layer). We used the G band (~1580 cm^{-1}) intensity to calculate the enhancement ratio of Raman signals on different substrates and found that the enhancement ratio of Raman signal of monolayer graphene on Si/Ag/Al_2O_3 is ~5 compared with that on Si/Al_2O_3. It is needed to point out that this enhancement ratio varies from one sample to another and can reach ~20. Note that monolayer graphene is almost invisible on the substrates of Si/50 nm Ag and original Si wafer, thus it is very difficult to locate them for Raman measurements. Normally, the Raman signals of few-layer graphene are stronger than those of monolayer graphene, so the intensity of monolayer graphene on the original Si substrate should be much weaker than that of few-layer graphene shown in Figure 3. Therefore, we speculate that the enhancement ratio of monolayer graphene on Si/Ag/Al_2O_3 to the original Si substrate and Si/50 nm Ag substrate can reach the order of 10^3 and 10^2, respectively. Moreover, we found that, if the sandwiched metal layer in the SMO substrate is not SERS-active, such as Ti, Al, *etc.*, the Raman intensity of graphene is not enhanced at all com-
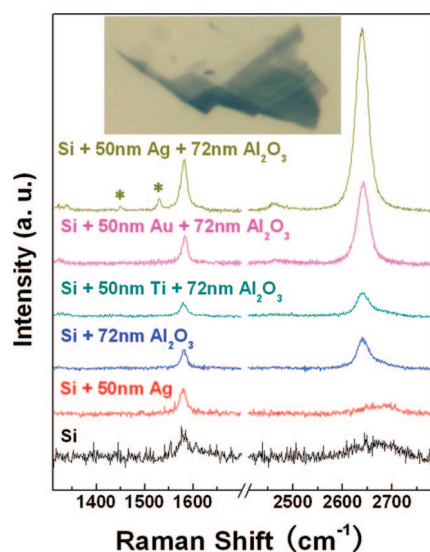

Figure 3. Raman spectra of graphene on different kinds of substrates. For original Si (without oxide layer) and Si/50 nm Ag substrates, the Raman spectra of few-layer ($<$5) graphenes instead of monolayer graphene were presented and taken at a laser power of about 10 mW and collection time of 1800 s and laser power of about 1 mW and collection time of 1200 s, respectively, since the monolayer graphene on these two substrates is nearly invisible and it is difficult to locate them for Raman measurements. For the other substrates, the Raman spectra were taken at a laser power of about 1 mW and a shorter collection time of 120 s. It reveals that the enhancement is different for different substrates, and the Raman signals of monolayer graphene are dramatically enhanced on the SMO substrates (Si/Ag/Al_2O_3 and Si/Au/Al_2O_3) compared with those on an IERS substrate of Si/Al_2O_3, or on a typical SERS substrate of Si/Ag and on an original Si wafer. Note that if the sandwiched metal layer, such as Ti, in a SMO substrate is not SERS-active, the Raman signals of graphene are not enhanced compared with the corresponding IERS substrate. The inset is the optical image of graphene on this Si/Ag/Al_2O_3 substrate.

pared with the corresponding IERS substrate. These results indicate that a remarkably enhanced Raman signal can be achieved for the graphene on a SMO substrate and further prove that both SERS and IERS processes are involved in this Raman scattering process.

Besides the enhanced Raman signals, the visibility of graphene is another prerequisite for its detailed structural characterization by using a nondestructive optical method, which allows one to easily search for and locate the studying samples. From this point, the substrates of Si and Si/50 nm Ag are also not suitable for Raman measurements of graphene (see Supporting Information). We calculated the total color difference of graphene on the optimized SMO substrate (see Supporting Information), and it is interesting to find that the graphene on the SMO substrate is visible in white light (see the inset of Figure 3). Consequently, the graphene can be easily located on the SICERS substrate during Raman measurements. The visibility of graphene on this novel sandwich-like SMO substrate is another important feature of our SICERS technique.

Figure 4a,b shows the Raman spectra of graphene with different layers on a typical SMO substrate (Si/50
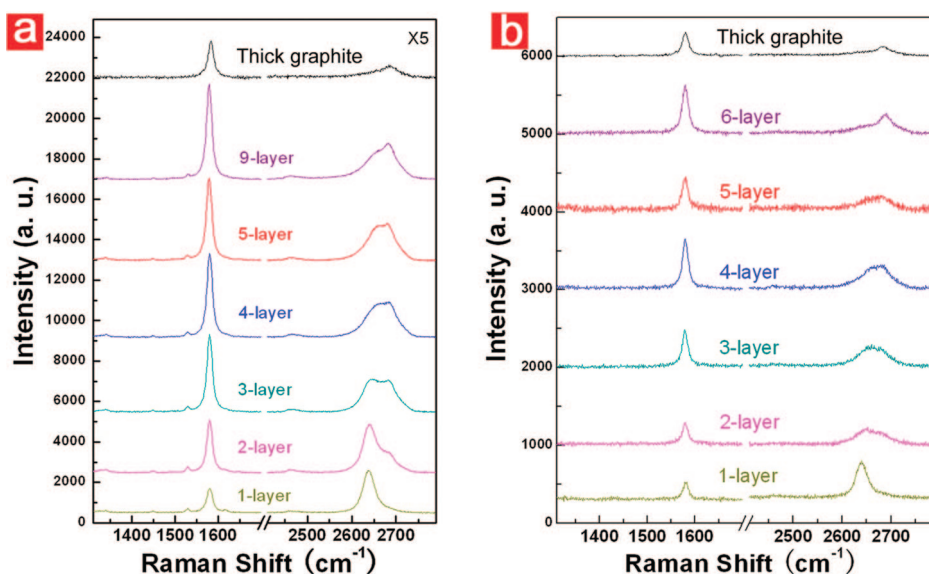
Figure 4. Raman spectra of graphene with different layers on SICERS and IERS substrates. (a) Raman spectra of graphene on a SICERS substrate of Si wafer capped with a 50 nm thick Ag layer and a 72 nm thick Al_2O_3 layer, and (b) Raman spectra of graphene on an IERS substrate of Si wafer capped with only a 72 nm thick Al_2O_3 layer, which were taken at a laser power of about 1 mW and short collection time of 120 s. They reveal that the enhancement on the SICERS substrate is obvious for mono-, bi-, and few-layer graphene but not for thick graphite, compared with that on the IERS substrate. The intensity of thick graphite keeps similar for the SICERS (G band intensity = 350) and IERS (G band intensity = 330) substrates.

nm Ag/72 nm Al_2O_3) and its corresponding IERS substrate (Si/72 nm Al_2O_3), respectively. It can be found that all the SICERS features, such as the peak position, line shape, and line width of G band and 2D band, keep similar to the IERS features.[10−12] However, all the Raman signals of mono-, bi-, and few-layer graphenes are dramatically enhanced on the SMO substrate, compared to those on the IERS substrate. Interestingly, if graphene layers are too thick (>20 layers, like thick graphite), the enhancement effect disappears. These results indicate that the SICERS is a general and effective technique for the remarkable enhancement of Raman signals of few-layer graphene. Another interesting phenomenon we should note is that the G band intensity of thick graphite is at least 10 times weaker than those of few-layer graphene on an SMO substrate and is in the same order of those of few-layer graphene on an IERS substrate. Since the intensity of thick graphite on different substrates keeps almost identical, it can be used as an intensity standard to evaluate the relative enhancement ratio.

Because of the remarkable enhancement in Raman signal intensity, the SICERS effect can be applicable for the characterization of the detailed structure of graphene, such as defects, edge structures, and doping. Here, we demonstrate the use of SICERS technique to probe the tiny structure change of graphene. Figure 5a shows the Raman spectra of graphene on an SMO substrate of the Si/50 nm Ag/72 nm Al_2O_3 obtained by mapping along the color bar in Figure 5b. As the Raman mapping locations change from blue to green, the SICERS spectra exhibit typical features of few-layer

(marked by blue), monolayer (marked by red), and bilayer (marked by green) graphene, including the line shape and frequency. Therefore, we suggest that the edge of this graphene is bilayer, as illustrated in Figure 5c. This structure is similar to that obtained by high-resolution transmission electron microscope observations.[37] From optical microscope (Figure 5b) and scanning electron microscope (see Figure S2, Supporting Information) observations, it is worth noting that the measured edge region is quite different from the inner region by color, which is ~100 nm in width. This confirms the edge structure obtained by Raman spectroscopy. However, we should note that, because there is only a small difference between the edge and inner region, the IERS Raman spectra of the edge and inner region should be almost the same or cannot be well-distinguished since the contribution of the difference is too small to change the weak Raman signals of graphene. The observed clear Raman signals of bilayer graphene at the edge indicate that the SICERS technique is helpful to accurately probe the tiny structure change due to the stronger Raman signals.

As another example, we investigated the surface structure of graphene prepared by micromechanical cleavage by utilizing SICERS technique and obtained some detailed information that cannot be easily obtained from conventional Raman scattering. Figure 6a,b shows the atomic force microscope (AFM) images of graphene on IERS and SICERS substrates, respectively. The topographic profiles indicate that the surface of graphene is not smooth with some fragments or ribbons, which is possibly attributed to the little difference of cleavage technique and raw material compared to that previously reported by another group.[38] Figure 6c shows the Raman spectra of graphene on the IERS and SICERS substrates, collected from the regions marked by circles in Figure 6a,b. The Raman spectrum (green line) of graphene on the IERS substrate remains similar to those previously reported in the literature for the defect-containing graphene or the edge region of graphene,[11,14] which generally include a G band, D band, and 2D band. However, after using longer collection time (360 s) and stronger laser (~5 mW), two new peaks appears at about 1450 and 1530 cm^{-1} (also see those indicated by * in Figure 3), although their intensities are very weak compared
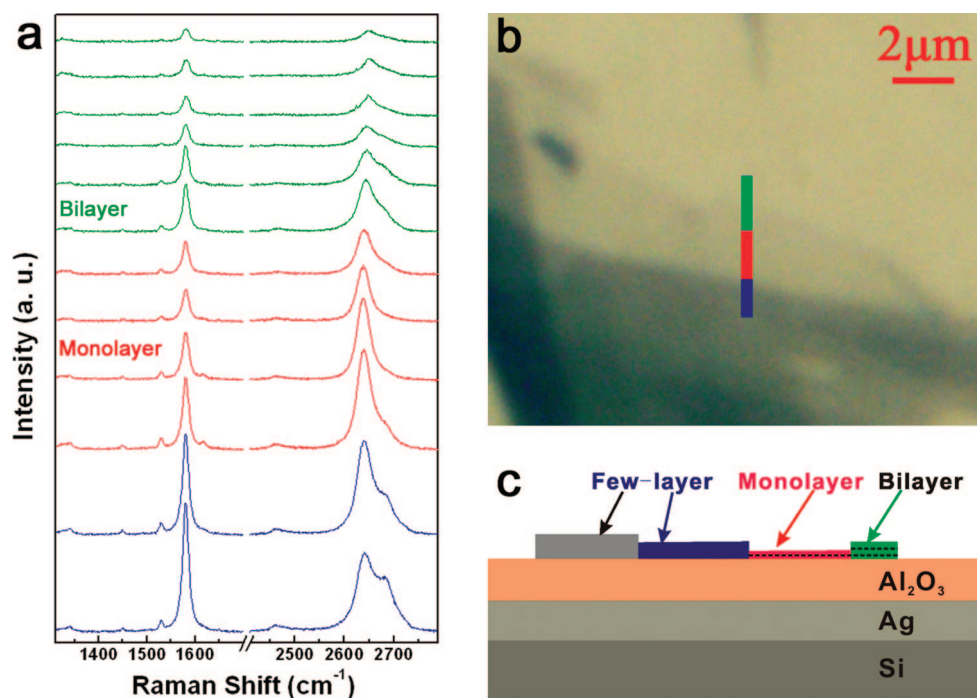
Figure 5. Morphology of graphene on an SMO substrate obtained from SICERS mapping. (a) SICERS mapping of graphene on the SMO substrate of Si/50 nm Ag/72 nm Al$_2$O$_3$, revealing that the number of graphene layers changes at different positions, and Raman feature of bilayer graphene appears at the edge. (b) Corresponding optical image of graphene, and the color bar corresponds to the different positions of SICERS mapping. (c) Schematic illustration of graphene on the SMO substrate deduced from SICERS mapping, showing that the number of graphene layers changes at the edge.

with the G band. Here, it is worth noting that these two peaks can be well-distinguished in the Raman spectra of graphene on the SICERS substrate taken with a low laser power of about 1 mW and short collection time of 120 s, besides a G band enhancement ratio of ~10. The appearance of these two peaks for the graphenes both on SICERS and IERS substrates reveals that they are not the SERS-induced. Combined with the fact that these two peaks are suppressed in smooth graphene (Figure S3, Supporting Information), we suggest that these two peaks are possibly related to the vibrations of fragments or ribbons on the surface of graphene. From the above, we can see that the SICERS technique is very sensitive to probe the detailed structure of graphene, which will be very helpful for its applications, especially in nanoelectronics.

CONCLUSIONS

We proposed a novel surface and interference coenhanced Raman scattering technique, combining surface-enhanced and interference-enhanced Raman scattering mechanisms, to dramatically enhance the Raman signals of graphene by using a specifically designed substrate of

Si/SERS active metal/oxide layer. An enhancement ratio in the order of 10^3 can be achieved by optimizing the substrate structure. Another important feature of this method is that graphene is visible and can be easily located in white light on this specific substrate. Due to the high structural sensitivity, fine structural informa-
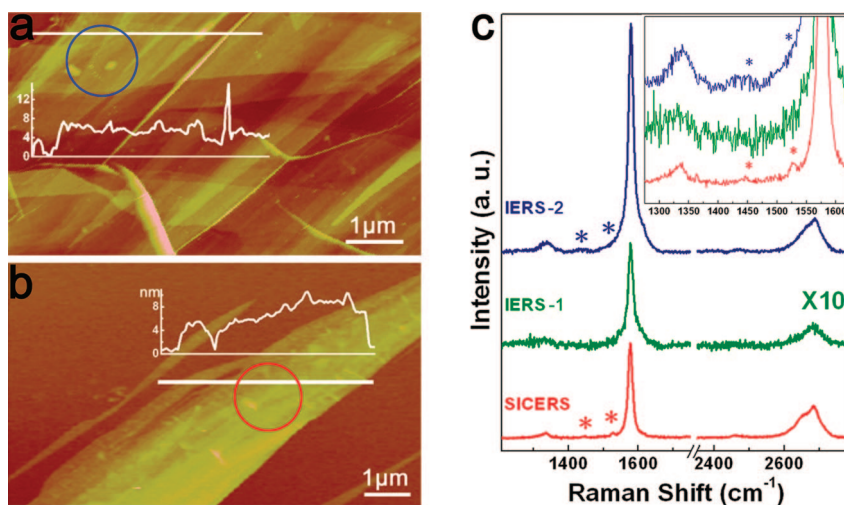

Figure 6. AFM images of graphene (a) on an IERS substrate (Si/285 nm SiO$_2$) and (b) on a SICERS substrate (Si/80 nm Ag/72 nm Al$_2$O$_3$). The inset shows the cross-section measurements taken along the white line, indicating the presence of some fragments or ribbons. The circles denote the Raman measurement positions. (c) Raman spectra of graphene on the IERS (green and blue lines) and SICERS (red line) substrates, which were collected from the regions marked by squares shown in (a) and (b), respectively. IERS-1 (green line) and SICERS were taken at a laser power of about 1 mW and collection time of 120 s, and IERS-2 (blue line) was taken at a laser power of about 5 mW and collection time of 360 s. The inset shows the details of two additional peaks about 1450 and 1530 cm^{-1}.

tion of graphene, such as the tiny structure change and surface structure of graphene, can be easily probed. This technique makes Raman spectroscopy a more powerful tool and opens up exciting opportunities in the field of ultrasensitive characterization of graphene, time-dependent structural evolution investigation, and characterization of graphene-based nanoelectronics with high spatial resolution.

EXPERIMENTAL SECTION

The graphene samples were prepared by micromechanical cleavage of highly oriented pyrolytic graphite (HOPG) with scotch tape and then transferred to the substrates.[38] Si wafers capped with different kinds and thicknesses of dielectric films were made by a film-coating system (Gatan Model 682 precision etching coating system) as follows. First, Si substrates were cleaned and loaded on the sample holder. After the chamber was pumped to the working pressure (4×10^{-3} Pa), the ion gun voltage and ion beam current were turned on, and then different kinds of coating materials, such as Ag, Au, Ti, Al_2O_3, and SiO_2, were deposited on the Si surface at a steady deposition rate. The film thickness was *in situ* recorded by a quartz crystal. The Raman spectra were measured and collected using 632.8 nm laser with JY HR800 under ambient conditions, with a laser spot size of about 1 μm. For the Raman measurements of few-layer graphene on original Si substrate and Si substrate capped with a 50 nm Ag film and a 160 nm Al_2O_3 film, we adopted a strong laser power (~10 mW) and longer collection time (1800 s) because of their weak Raman signals.

Supporting Information Available: Calculated total color difference of graphene on different substrates, SEM image of the graphene shown in Figure 5, and the Raman spectrum of smooth few-layer graphene on the SICERS substrate. This material is available free of charge *via* the Internet at http://pubs.acs.org.

REFERENCES AND NOTES

1. Novoselov, K. S.; Geim, A. K.; Morozov, S. V.; Jiang, D.; Katsnelson, M. I.; Grigorieva, I. V.; Dubonos, S. V.; Firsov, A. A. Two-Dimensional Gas of Massless Dirac Fermions in Graphene. *Nature* **2005**, *438*, 197–200.
2. Zhang, Y. B.; Tan, Y. W.; Stormer, H. L.; Kim, P. Experimental Observation of the Quantum Hall Effect and Berry's Phase in Graphene. *Nature* **2005**, *438*, 201–204.
3. Geim, A. K.; Novoselov, K. S. The Rise of Graphene. *Nat. Mater.* **2007**, *6*, 183–191.
4. Novoselov, K. S.; Geim, A. K.; Morozov, S. V.; Jiang, D.; Zhang, Y.; Dubonos, S. V.; Grigorieva, I. V.; Firsov, A. A. Electric Field Effect in Atomically Thin Carbon Films. *Science* **2004**, *306*, 666–669.
5. Schedin, F.; Geim, A. K.; Morozov, S. V.; Hill, E. W.; Blake, P.; Katsnelson, M. I.; Novoselov, K. S. Detection of Individual Gas Molecules Adsorbed on Graphene. *Nat. Mater.* **2007**, *6*, 652–655.
6. Stankovich, S.; Dikin, D. A.; Dommett, G. H. B.; Kohlhaas, K. M.; Zimney, E. J.; Stach, E. A.; Piner, R. D.; Nguyen, S. T.; Ruoff, R. S. Graphene-Based Composite Materials. *Nature* **2006**, *442*, 282–286.
7. Wang, F.; Zhang, Y. B.; Tian, C. S.; Girit, C.; Zettl, A.; Crommie, M.; Shen, Y. R. Gate-Variable Optical Transitions in Graphene. *Science* **2008**, *320*, 206–209.
8. Becerril, H. A.; Mao, J.; Liu, Z. F.; Stoltenberg, R. M.; Bao, Z. N.; Chen, Y. S. Evaluation of Solution-Processed Reduced Graphene Oxide Films as Transparent Conductors. *ACS Nano* **2008**, *2*, 463–470.
9. Wang, X.; Zhi, L. J.; Mullen, K. Transparent, Conductive Graphene Electrodes for Dye-Sensitized Solar Cells. *Nano Lett.* **2008**, *8*, 323–327.
10. Ferrari, A. C.; Meyer, J. C.; Scardaci, V.; Casiraghi, C.; Lazzeri, M.; Mauri, F.; Piscanec, S.; Jiang, D.; Novoselov, K. S; Roth, S.; Geim, A. K. Raman Spectrum of Graphene and Graphene Layers. *Phys. Rev. Lett.* **2006**, *97*, 187401.
11. Gupta, A.; Chen, G.; Joshi, P.; Tadigadapa, S.; Eklund, P. C. Raman Scattering from High-Frequency Phonons in Supported *n*-Graphene Layer Films. *Nano Lett.* **2006**, *6*, 2667–2673.
12. Graf, D.; Molitor, F.; Ensslin, K.; Stampfer, C.; Jungen, A.; Hierold, C.; Wirtz, L. Spatially Resolved Raman Spectroscopy of Single- and Few-Layer Graphene. *Nano Lett.* **2007**, *7*, 238–242.
13. Pimenta, M. A. Studying Disorder in Graphite-Based Systems by Raman Spectroscopy. *Phys. Chem. Chem. Phys.* **2007**, *9*, 1276–1291.
14. Ferrari, A. C. Raman Spectroscopy of Graphene and Graphite: Disorder, Electron-Phonon Coupling, Doping and Nonadiabatic Effects. *Solid State Commun.* **2007**, *143*, 47–57.
15. Casiraghi, C.; Pisana, S.; Novoselov, K. S.; Geim, A. K.; Ferrari, A. C. Raman Fingerprint of Charged Impurities in Graphene. *Appl. Phys. Lett.* **2007**, *91*, 233108.
16. Stampfer, C.; Molitor, F.; Graf, D.; Ensslin, K.; Jungen, A.; Hierold, C.; Wirtz, L. Raman Imaging of Doping Domains in Graphene on SiO_2. *Appl. Phys. Lett.* **2007**, *91*, 233108.
17. Das, A.; Pisana, S.; Chakraborty, B.; Piscanec, S.; Saha, S. K.; Waghmare, U. V.; Novoselov, K. S.; Krishnamurthy, H. R.; Geim, A. K.; Ferrari, A. C.; Sood, A. K. Monitoring Dopants by Raman Scattering in an Electrochemically Top-Gated Graphene Transistor. *Nat. Nanotechnol.* **2008**, *3*, 210–215.
18. Malard, L. M.; Nilsson, J.; Elias, D. C.; Brant, J. C.; Plentz, F.; Alves, E. S.; Castro, A. H.; Pimenta, M. A. Probing the Electronic Structure of Bilayer Graphene by Raman Scattering. *Phys. Rev. B* **2007**, *76*, 201401.
19. Calizo, I.; Balandin, A. A.; Bao, W.; Miao, F.; Lau, C. N. Temperature Dependence of the Raman Spectra of Graphene and Graphene Multilayers. *Nano Lett.* **2007**, *7*, 2645–2649.
20. Calizo, I.; Miao, F.; Bao, W.; Lau, C. N.; Balandin, A. A. Variable Temperature Raman Microscopy as a Nanometrology Tool for Graphene Layers and Graphene-Based Devices. *Appl. Phys. Lett.* **2007**, *91*, 071913.
21. Ni, Z. H.; Yu, T.; Lu, Y. H.; Wang, Y. Y.; Feng, Y. P.; Shen, Z. X. Uniaxial Strain on Graphene: Raman Spectroscopy Study and Band-Gap Opening. *ACS Nano* **2008**, *2*, 2301–2305.
22. Nair, R. R.; Blake, P.; Grigorenko, A. N.; Novoselov, K. S.; Booth, T. J.; Stauber, T.; Peres, N. M. R.; Geim, A. K. Fine Structure Constant Defines Visual Transparency of Graphene. *Science* **2008**, *320*, 1308.
23. Saito, R.; Dresselhaus, M. S.; Dresselhaus, G. *Physical Properties of Carbon Nanotubes*; Imperial College Press: London, 1998.
24. Wang, Y. Y.; Ni, Z. H.; Yu, T.; Shen, Z. X.; Wang, H. M; Wu, Y. H.; Chen, W.; Wee, A. T. S. Raman Studies of Monolayer Graphene: The Substrate Effect. *J. Phys. Chem. C* **2008**, *112*, 10637–10640.
25. Calizo, I; Bao, W. Z.; Miao, F.; Lau, C. N.; Balandin, A. A. The Effect of Substrates on the Raman Spectrum of Graphene: Graphene-on-Sapphire and Graphene-on-Glass. *Appl. Phys. Lett.* **2007**, *91*, 201904.
26. Calizo, I.; Teweldebrhan, D.; Bao, W.; Miao, F.; Lau, C. N.; Balandin, A. A. Spectroscopic Raman Nanometrology of Graphene and Graphene Multilayers on Arbitrary Substrates. *J. Phys.: Conf. Ser.* **2008**, *109*, 012008.

27. Gao, L. B.; Ren, W. C.; Li, F.; Cheng, H. M. Total Color Difference for Rapid and Accurate Identification of Graphene. *ACS Nano* **2008**, *2*, 1625–1633.

28. Blake, P.; Hill, E. W.; Neto, A. H. C.; Novoselov, K. S.; Jiang, D.; Yang, R.; Booth, T. J.; Geim, A. K. Making Graphene Visible. *Appl. Phys. Lett.* **2007**, *91*, 063124.

29. Nemanich, R. J.; Tsai, C. C.; Connell, G. A. N. Interference-Enhanced Raman Scattering of Very Thin Titanium and Titanium Oxide Films. *Phys. Rev. Lett.* **1980**, *44*, 273–276.

30. Connell, G. A. N.; Nemanich, R. J.; Tsai, C. C. Interference Enhanced Raman Scattering from Very Thin Absorbing Films. *Appl. Phys. Lett.* **1980**, *36*, 31–33.

31. Gupta, S.; Morell, G.; Katiyar, R. S.; Abelson, J. R.; Jin, H. C.; Balbert, I. Interference Enhanced Raman Scattering of Hydrogenated Amorphous Silicon Revisited. *J. Raman Spectrosc.* **2001**, *32*, 23–25.

32. Wang, Y. Y.; Ni, Z. H.; Shen, Z. X.; Wang, H. M.; Wu, Y. H. Interference Enhancement of Raman Signal of Graphene. *Appl. Phys. Lett.* **2008**, *92*, 043121.

33. Kneipp, K.; Wang, Y.; Kneipp, H.; Perelman, L. T.; Itzkan, I.; Dasari, R.; Feld, M. S. Single Molecule Detection Using Surface-Enhanced Raman Scattering (SERS). *Phys. Rev. Lett.* **1997**, *78*, 1667–1670.

34. Kneipp, K.; Kneipp, H.; Corio, P.; Brown, S. D. M.; Shafer, K.; Motz, J.; Perelman, L. T.; Hanlon, E. B.; Marucci, A.; Dresselhaus, G.; Dresselhaus, M. S. Surface-Enhanced and Normal Stokes and Anti-Stokes Raman Spectroscopy of Single-Walled Carbon Nanotubes. *Phys. Rev. Lett.* **2000**, *84*, 3470–3473.

35. Kneipp, K.; Kneipp, H.; Itzkan, I.; Dasari, R. R.; Feld, M. S. Surface-Enhanced Raman Scattering and Biophysics. *J. Phys.: Condens. Matter* **2002**, *14*, R597−R624.

36. Campion, A.; Kambhampati, P. Surface-Enhanced Raman Scattering. *Chem. Soc. Rev.* **1998**, *27*, 241–250.

37. Meyer, J. C.; Geim, A. K.; Katsnelson, M. I.; Novoselov, K. S.; Booth, T. J.; Roth, S. The Structure of Suspended Graphene Sheets. *Nature* **2007**, *446*, 60–63.

38. Novoselov, K. S.; Jiang, D.; Schedin, F.; Booth, T. J.; Khotkevich, V. V.; Morozov, S. V.; Geim, A. K. Two-Dimensional Atomic Crystals. *Proc. Natl. Acad. Sci. U.S.A.* **2005**, *102*, 10451–140553.

ARTICLE